Journal of the European Ceramic Society **16** (1996) 1277–1282

PII:S0955-2219(96)00053-2
0955-2219/96/$15.00

Subsolidus Phase Relationships in the System Dy_2O_3–Si_3N_4–AlN–Al_2O_3

W. Y. Sun,[a] D. S. Yan,[a] L. Gao,[a] H. Mandal[b] & D. P. Thompson[b]

[a] The State Key Lab on High Performance Ceramics and Superfine Microstructure, Shanghai Institute of Ceramics, Academia Sinica, Shanghai, People's Republic of China
[b] Wolfson Laboratory, Materials Division, Department of Mechanical, Materials & Manufacturing Engineering, University of Newcastle upon Tyne, UK

(Received 20 November 1995; revised version received 20 February 1996; accepted 28 February 1996)

Abstract

Subsolidus phase relationships in the system Dy–Si–Al–O–N have been determined. Forty-two compatibility tetrahedra were established in the region Dy_2O_3–Si_3N_4–AlN–Al_2O_3. Within this region, DyAG($Dy_3Al_5O_{12}$) and M'-phase ($Dy_2Si_{3-x}Al_xO_{3+x}N_{4-x}$) are the only two important compounds which have tie lines joined to β-sialon and AlN polytypoid phases. α-Sialon coexists with both M' phase and DyAG (only with oxygen-rich α'). Copyright © 1996 Elsevier Science Ltd

1 Introduction

The importance of using rare earth oxides for the densification of silicon nitride ceramics has been recognised in recent years. Not only are they very effective along with alumina for densification, either singly or in combination with yttria, but they can also be accommodated in the α-Si_3N_4 lattice forming α-sialon (α-Si_3N_4 solid solution with the composition $Ln_xSi_{12-(m+n)}Al_{m+n}O_nN_{16-n}$, also called α'), thus providing an opportunity for decreasing the transient liquid phase content after sintering and hence reducing the amount of residual grain boundary glass. Therefore, phase relationships in Ln–Si–Al–O–N systems are of particular interest.

It is known that elements in the lanthanide (Ln) series are similar to yttrium in compound formation and phase relationships. Previous work on Ln–Si–O–N subsystems,[1] indicates that the phase relationships are nearly the same as in the Y–Si–O–N system, but in Ln–Al–O–N systems[2] the phase relationships vary with the atomic number of the rare earth element. The phase relationships in systems with high Z-value of the rare earth element are similar to those in Y–Al–O–N.[3] In the systems Ln–Al–O–N (where Ln = Ce → Sm) two N-containing compounds exist — Ln_2AlO_3N and $Ln_2Al_{12}O_{18}N_2$ (magneto-plumbite, MP compound) — and no garnet phase occurs; instead, the aluminate with 1 : 1 becomes stable.[2] The Ln_2AlO_3N and MP compounds do not occur in those systems containing rare earth oxides with cations smaller than that of Gd.[2,4] Therefore, in the five-component systems with low Z-value rare earth elements, the phase relationships become a little bit different from those in Y–Si–Al–O–N.[5–7] In the oxygen-rich region where two five-component phases[8,9] — U-phase ($Ln_3Si_{3-x}Al_{3+x}O_{12+x}N_{2-x}$) and W-phase ($Ln_4Si_9Al_5O_{30}N$) — exist, the former is stable for rare earth cations between La and Dy and the latter stable only in La, Ce and Nd systems. Recent work on Ln-melilite[10,11] indicates that the formation of melilite solid solution ($Ln_2Si_{3-x}Al_xO_{3+x}N_{4-x}$) occurs easily for melilite containing light rare earth elements and that the top solubility limit of Al and O decreases with increasing Z-value (x = 1 for Nd and x = 0·6 for Er). In recent years, work has focused on the Sm(or Nd)–Si–Al–O–N system.[12,13] The results indicate Nd has the same behaviour as Sm: below the subsolidus temperatures Nd(Sm)AlO_3 coexists with β-sialon (β-Si_3N_4 solid solution, $Si_{6-z}Al_zO_zN_{8-z}$, β') and all AlN polytypoids and α-sialon can only be compatible with melilite solid solution. Dysprosium is one of the central elements in the rare earth series; in this region, phase relationships in Ln–Si–Al–O–N systems are changing from those observed for the low-Z elements (La, Nd, Sm) to those observed for the high-Z elements (Er, Yb... and Y). Studies on the Dy–Si–Al–O–N system will therefore give an indication of whether these changes occur simultaneously or whether there is overlap in this region between the different phase relationships observed for the high-Z and low-Z

regimes. To elucidate the variation of phase relationships in the Ln–Si–Al–O–N system with rare earth element and to study the Dy–Si–Al–O–N system itself, the aim of the current work is to determine the subsolidus phase relationships in the region defined by the four end-members Si_3N_4, AlN, Al_2O_3 and Dy_2O_3 (Fig. 1). This region includes the phases α-sialon, β-sialon and AlN polytypoids, and covers the range of compositions used for the design and processing of commercial multi-phase sialon ceramics.

2 Experimental Procedure

The present paper is the result of two work programmes carried out separately at Shanghai Institute of Ceramics and the University of Newcastle upon Tyne. The symbol * is used to represent the experiments carried out at Newcastle. The starting powders used were α-Si_3N_4 (Starck H1 and Starck LC10*), AlN (supplied by Zhuzhou Institute of Hard Metal Alloys, containing 1·2% oxygen and Starck Grade B*), Al_2O_3 (99·99%, produced by decomposing ammonium alum and Alcoa A17*), Dy_2O_3 (99·9%, Yaolung Chemical Works, China and 99·9%, Aldrich Chemical Co. Ltd*). The oxygen contents of the nitride powders were taken into account in calculating compositions. The starting powders were weighed out and ground in absolute alcohol or isopropanol* using an agate pestle and mortar. The mixed powders were dried, pressed into pellets 10 mm in diameter and then isostatically pressed under a pressure of 200 MPa. The specimens prepared at Shanghai were fired in a graphite-resistant furnace with a rather slow cooling rate (~ 50°C min^{-1}), whilst those at Newcastle were fired in graphite-resistant furnace which could be cooled down to room temperature very quickly (~ 100°C min^{-1}). A nitrogen atmosphere was used in all cases. The specimens with compositions near liquid-phase region were heat-treated after firing. All specimens were examined by X-ray diffractometry or using a Hägg–Guinier focusing camera. Only specimens showing less than 3% weight loss after firing were used for data analysis.

3 Results and Discussion

Twenty-three compositions in the region bounded by Si_3N_4, AlN, Al_2O_3 and Dy_2O_3 were studied to establish compatibility relationships. The binary tie lines established were based on the results listed in Table 1. Based on the much more extensive knowledge of phase relationships in the Y–Si–Al–O–N and Sm(Nd)–Si–Al–O–N systems and other information in the literature listed above, 42 compatibility tetrahedra were established in this region (Table 2). In the present work α-sialon is considered as a point composition and its detailed solid solution range has not been determined.

As indicated in this table, DyAG($Dy_3Al_5O_{12}$) is a stable phase and is compatible with all the AlN polytypoid phases, β-sialon (from β_{10} to β_{60}) and α-sialon (oxygen-rich), forming 12 AlN-polytypoids-containing compatibility tetrahedra (Fig. 2) and one α'-β'-containing compatibility tetrahedron, α'-β_{10}–DyAG–12H (Fig. 3). M' was also found to have tie lines with β-sialon from

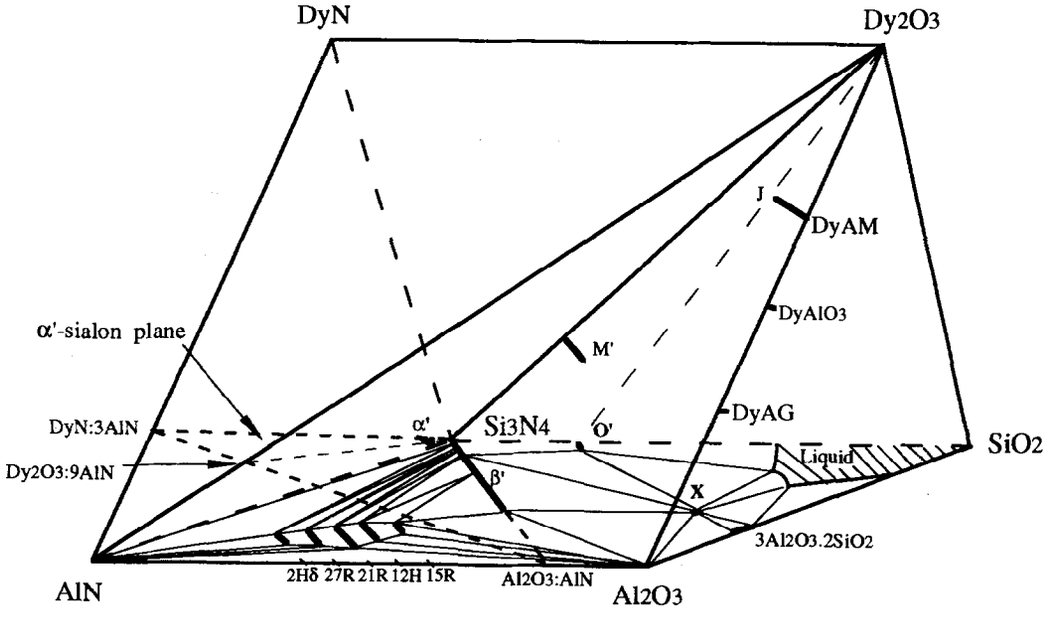

Fig. 1. Representation of Dy-SiAlON system showing phases occurring in the region bounded by Si_3N_4, Dy_2O_3, Al_2O_3 and AlN, and Si–Al–O–N behaviour diagram at 1700°C (α-sialon plane = the plane with α-sialon composition $Dy_xSi_{12-(m+n)}Al_{m+n}O_nN_{16-n}$).

Table 1. Compositions studied in the system Si_3N_4-AlN–Al_2O_3–Dy_2O_3

No.	Composition (wt%)				Firing (°C–h)	Phases present[a]	Heat treatment (°C–h)	Phases present[a]
	Si_3N_4	AlN	Al_2O_3	Dy_2O_3				
1*	80·52	2·74	2·92	13·83	1750–1	β(s); M' (w)	1350–24 1550–5^	β (s); M' (m); DyAG (w) β (s); M' (m)
2	77·70	5·14	2·55	14·62	1800–1	β (s); M' (w)	1350–24	β (s); M' (m); DyAG (w)
3*	73·43	6·09	5·86	14·61	1750–1	β' (s) ; α' (m)	1550–24 1550–5^	β' (s); α' (mw); DyAG (m); M' (w) β' (s); α' (w); M' (m)
4	70·00	0·00	6·44	23·56	1800–1	β (s); M' (s)	1350–24 1550–5^	β (ms); M' (m); DyAG (w) β (ms); M' (m)
5	69·39	5·53	11·26	13·81	1750–1	β' (s); α' (m); 21R (m)	1350–24	β_{10} (s); DyAG (s)
6	63·75	6·82	15·16	13·74	1800–1	α' (m); β' (m); 21R (s)	1350–24	β_{10} (s); DyAG (s)
7	53·22	9·85	23·13	13·80	1700–1	β' (s); 15R (vw)	1350–24	β_{20} (s); DyAG (s)
8	49·88	9·24	21·18	19·70	1750–1	β' (s); 15R (vw)	1350–24	β_{20} (s); DyAG (s)
9	49·69	10·88	11·71	27·72	1750–1	α' (m); β' (w); K(m)	1350–24 1550–5	DyAG (s); α' (m); β' (w); K (w?) DyAG (s); α' (m); β' (w); K (w?)
10*	38·43	31·97	11·03	18·58	1800–1	α'(m); 21R (m)	1350–24 1550–5	α' (m); 21R (m) α' (m); 21R (m); M'(m)
11*	35·38	29·34	17·49	17·79	1800–1	12H (ms); α' (m); β' (w)	1350–24 1550–5	12H (m); α' (m); DyAG (m); β' (w) 12H (m); α' (m); DyAG (m); β' (w)
12	16·05	1·29	1·87	80·78	1700–1	M' (x = 0·3) (s); J' (x = 1) (ms)		
13	13·30	1·29	4·87	80·56	1700–1	M' (x = 0·75) (s); J' (x = 1·4) (w)		
14	11·28	37·05	13·85	37·80	1700–1	M' (s); DyAG (s); 21R (m)		
15	11·14	—	—	88·86	1700–1	J (s)		
16	7·80	—	3·61	88·59	1700–1	J' x = 0·6) (s)		
17	7·64	32·40	23·13	36·83	1700–1	DyAG (s); 21R (w)		
18	6·28	0·77	19·60	73·35	1600–1	DyAG (s); M' (ms); DyAP (w); (J' (w)		
19	6·28	0·77	12·85	80·10	1650–1	J' (x = 1·4) (m); DyAP (m); M' (w)		
20	5·57	—	6·01	88·42	1700–1	J' (x = 1) (s)		
21	3·34	—	8·42	88·24	1700–1	J' (x = 1·4) (s)		
22	1·67	30·00	1·80	66·53	1550–1	Dy_2O_3(s); J' (x = 0·6) (s) AlN (m)		
23	0·84	40·00	9·14	50·02	1600–1	DyAP; (s); J' (x=1) (m) AlN (m)		

[a] α = α – Si_3N_4; α' = α-sialon ($Ln_xSi_{12-(m+n)}Al_{m+n}O_nN_{16-n}$); β = β-Si_3N_4; β', β_{10}, β_{20}... = β-sialon (β_{10}, β_{20} ≈ β' with z = 0·8, 1·5, $Si_{6-z}Al_zO_zN_{8-z}$); DyAp = $LnAlO_3$; M' = $Dy_2Si_{3-x}Al_xO_{3+x}N_{4-x}$ (x = 0 → 0·75); J' = $Dy_4Si_{2-x}Al_xO_{7+x}N_{2-x}$ (x = 0 → 2); K = $Dy_2Si_2O_4N_2$; s = strong; m = medium; mw = medium weak; ms = medium strong; vw = very weak.

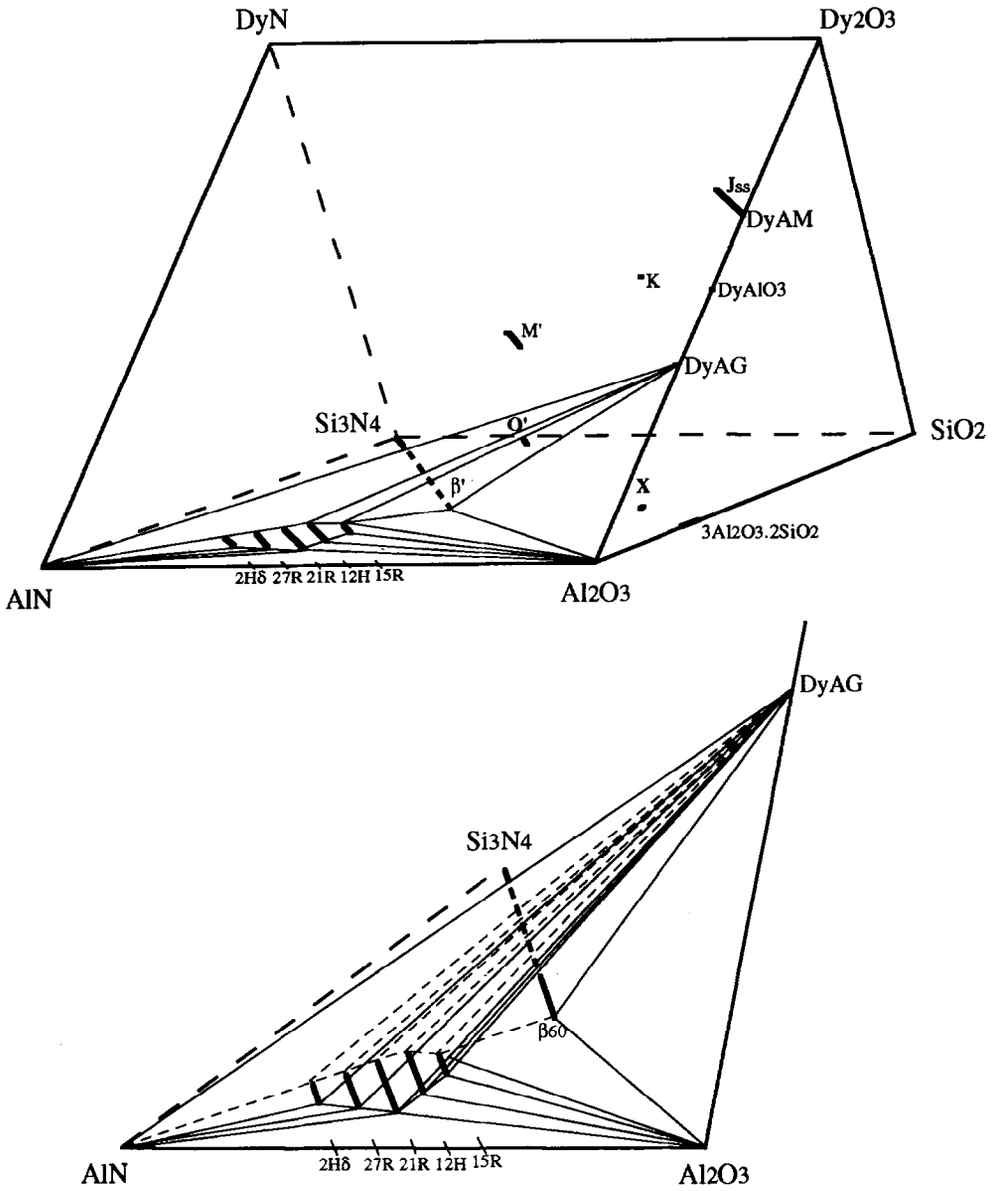

Fig. 2. DyAG($Dy_3Al_5O_{12}$) is compatible with Al_2O_3, all polytypoid phases and AlN forming 12 compatibility tetrahedra: DyAG–β_{60}–15R–Al_2O_3,DyAG–15R–Al_2O_3, DyAG–15R–12H, DyAG–12H–21R, DyAG–21R–27R, DyAG–27R–$2H^{\delta}$, DyAG–$2H^{\delta}$–AlN, DyAG–$2H^{\delta}$–AlN–27R, DyAG–27R–AlN–21R,DyAG–21R–AlN–Al_2O_3, DyAG–21R–Al_2O_3–12H and DyAG–12H–Al_2O_3–15R.

$\beta_0(\beta$–$Si_3N_4)$ to β_{10} and α', forming two α'–β'-containing compatibility tetrahedra: α'–β_0–β_{10}–M' (Fig. 4) and α'–β_{10}–M'–DyAG. $Dy_4Si_2O_7N_2$ (J-phase) also forms a continuous solid solution with $Dy_4Al_2O_9$ in a way similar to $Y_4Si_2O_7O_2$. In the Y–Si–Al–O–N system, the variation of unit cell dimensions (monoclinic) of J'-phase (solid solution of J-phase) with composition is not linear and the compositions near the centre of the range have simple X-ray patterns which index on a tetragonal unit cell related to the monoclinic cell.[5] A similar variation of unit cell dimensions also occurs for Dy-J'-phase. The X-ray patterns of the compositions near $x = 1{\cdot}4$ ($Dy_4Si_{2-x}Al_xO_{7+x}N_{2-x}$) can index on both tetragonal and monoclinic unit cells. The variation of the unit cell dimensions of Dy-J' phase will be further determined and published elsewhere. The compound $DyAlO_3$ was found to be compatible only with M' (melilite solid solution) and Si-rich terminals of AlN polytypoids (from AlN to 21R). The tie line between β' and $LnAlO_3$ that occurs in the Nd(Sm)–Si–Al–O–N systems does not exist in the Dy–Si–Al–O–N system.

In the region studied, DyAG, $DyAlO_3$, M'-phase and J'-phase were the main Dy-containing stable phases observed. In the Si_3N_4-rich compositions, DyAG phase could only be observed in the specimens after post-sintering heat treatment at a temperature around 1350°C and M'-phase was also observed to increase in post-sintering heat treatment around 1550°C. With the crystallization of DyAG and M'-phase during heat-treatment, the α-sialon, which was not expected to occur in these compositions, transformed into β'-sialon. Therefore, in establishing subsolidus phase relationships, judgement of the correct equilibrium

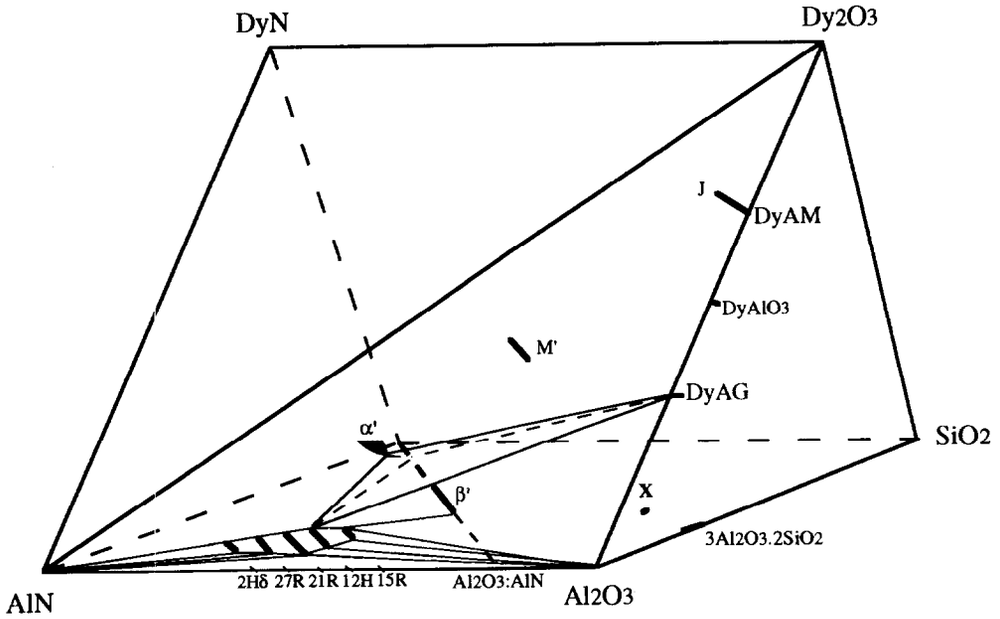

Fig. 3. DyAG($Dy_3Al_5O_{12}$) is compatible with β-sialon (β_{10}–β_{60}) and α-sialon (oxygen-rich) forming α'–β_{10}–12H–DyAG compatibility tetrahedron.

phases under subsolidus temperature conditions can sometimes be a difficult problem. Using phase assemblages observed at the same temperature for all conditions studied might lead to mistaken results, since different compositions may need different temperatures to fully crystallize the liquid phase. In the present work, all starting compositions were designed to fall on supposed tie lines or into supposed compatibility triangles. For example, compositions Nos 2 and 3 were on the lines between M' ($Ln_2Si_2AlO_4N_3$) and β-sialon (β_5 and β_{10}) and Nos 1, 5, 6 and 7 were designed on the composition lines between DyAG and β-sialon (β_0, β_{10} and β_{15} and β_{30}, respectively). If the expected phases were obtained after heat-treatment under a particular set of conditions, then equilibrium was believed to have been achieved. Based on this philosophy, compositions marked with the symbol ^ in Table 1, i.e. compositions Nos 1, 3, and 4, were believed to have achieved equilibrium and were used to establish the subsolidus phase relationships. In the compositions 3,5 and 6, the expected phases are β' with DyAG (Nos 5 and 6) or M'-phase (No. 3). These phase assemblages could only be achieved in post-sintering heat-treatment. The occurrence of α-sialon as a transitional phase can be attributed to the kinetic priority in the formation of Dy–α-sialon over the formation of DyAG and M'-phase at high temperatures. In heat treatment the DyAG and M'-phase is crystallized out at the exhaustion of Dy content in the liquid phase, thus making α-sialon transform

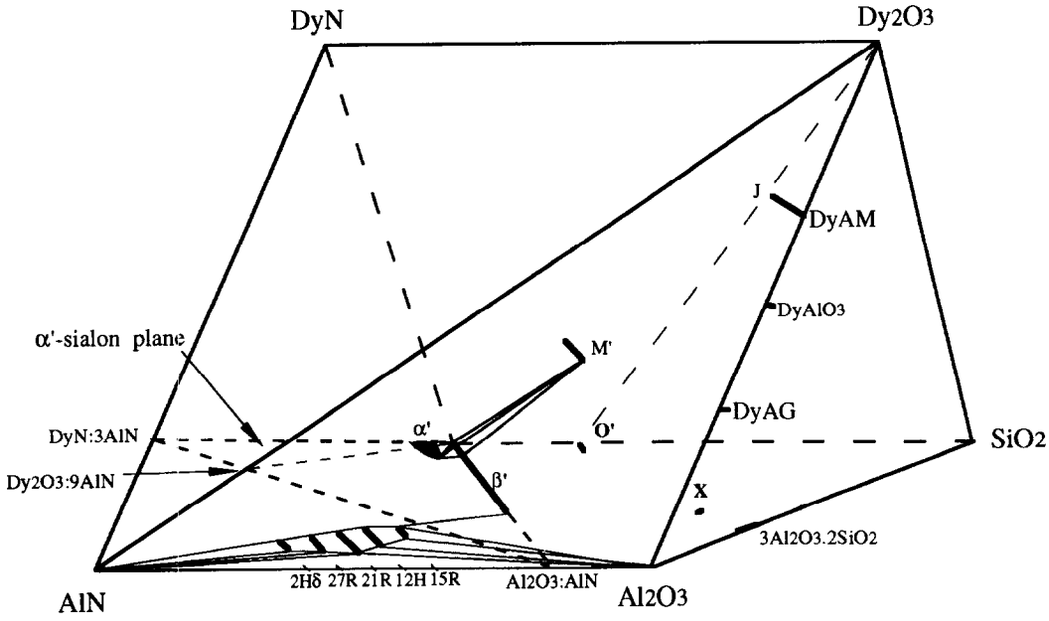

Fig. 4. M' (melilite solid solution) is compatible with β-sialon (β_0–β_{10}) and α-sialon forming α'–β'–M' compatibility tetrahedron.

Table 2. Subsolidus compatibility tetrahedra in the systems Si_3N_4–AlN–Al_2O_6–Dy_2O_3

Al_2O_3–β_{60}–15R–DyAG	Al_2O_3–15R–15R'–DyAG
Al_2O_3–15R'–12H'–DyAG	Al_2O_3–12H'–21R'–DyAG
Al_2O_3–21R'–AlN–DyAG	15R–15R'–12H–12H'–DyAG
12H–12H'–21R–21R'–DyAG	21R–21R'–27R–27R'–DyAG
27R–27R'–$2H^{\delta}$–$2H^{\delta*}$–DyAG	$2H^{\delta}$–$2H^{\delta*}$–AlN–DyAG
21R'–27R'–AlN–DyAG	27R'–$2H^{\delta*}$–AlN–DyAG
β_{60}–β_{25}–15R–DyAG	β_{25}–15R–12H–DyAG
β_{25}–β_{10}–12H–DyAG	β_{10}–12H–21R–α'
21R–β_{10}–β_8–α'	β_8–21R–27R–α'
27R–β_8–β_5–α'	β_5–27R–$2H^{\delta}$–α'
$2H^{\delta}$–β_5–β_2–α'	β_2–$2H^{\delta}$–AlN–α'
AlN–β_2–β_0–α'	β_0–β_{10}–α'–M'
β_{10}–12H–α'–DyAG	12H–21R–α'–DyAG
21R–27R–α'–M'	27R–$2H^{\delta}$–α'–M'
$2H^{\delta}$–AlN–α'–M'	AlN–$2H^{\delta}$–M'–DyAP
$2H^{\delta}$–27R–M'–DyAP	27R–21R–M'–DyAP
AlN–$2H^{\delta}$–YAP–DyAG	$2H^{\delta}$–27R–DyAP–DyAG
27R–21R–YAP–DyAG	21R–M'–DyAG–DyAP
21R–α'–M'–DyAG	α'–β_{10}–DyAG–M'
J' (middle)–DyAM–DyAP–AlN	Dy_2O_3–J' (whole)–AlN
J–J' (middle)–M–M'–AlN	J' (middle)–M'–DyAP–AlN

DyAM = $Dy_4Al_2O_9$; DyAP=$DyAlO_3$; DyAG = $Dy_3Al_5O_{12}$; 15R, 12H, 21R, 27R, $2H^{\delta}$ are Si-rich terminals of AlN polytypoids; 15R', 12H', 21R', 27R', $2H^{\delta*}$ are Al-rich terminals of AlN polytypoids, for others see Table 1.

into β-sialon to achieve the subsolidus phase equilibrium. Our current work on $\alpha' \rightleftharpoons \beta'$ phase transformation in the Ln–Si–Al–O–N systems during heat-treatment shows that, besides the liquid phase which assists the transformation,[14] there still exist other effects, especially for Ln-α-sialons with low Z-values. Of the 42 compatibility tetrahedra established in the present work, the following five—which involve α–β-sialon and AlN polytypoids (which could be used as reinforcement phase for α', β' or α'–β' because of its fibre-like morphology) and the promising grain boundary phases DyAG and M'—are the most useful for the design of multiphase sialon ceramics. They are α-sialon–β_0–β_{10}–M'; α-sialon–β_{10}–M'–DyAG; α-sialon–β_{10}–DyAG–12H; α-sialon–12H–21R–DyAG; and β_{10}–β_{25}–12H–DyAG.

4 Conclusions

Subsolidus phase relationships in the system Dy_2O_3–Si_3N_4–AlN–Al_2O_3 have been determined. Forty-two compatibility tetrahedra have been established in this region. DyAG coexists with β-sialon, approximately from β_{10} (z = 0·8) to β_{60} (z = 4), α' (oxygen-rich composition) and all AlN polytypoids. The coexistence of M' with β-sialon is restricted to the range β_0–β_{10}. α-Sialon is also compatible with M'. The compatibility tetrahedra α-sialon–β_0–β_{10}–M', α-sialon–β_{10}–M'–DyAG, α-sialon–β_{10}–DyAG-12H, α-sialon–12H–21R–DyAG and β_{10}–β_{25}–12H–DyAG are the most useful for the design and processing of multiphase sialon ceramic materials.

Acknowledgements

This work was supported by NNSF (National Natural Science Foundation, China, contract number 59482001) and the Royal Society, UK.

References

1. Mitomo, M., Izumi, F., Horiuchi, S. & Matsui, Y., Phase relationships in the system Si_3N_4–SiO_2–La_2O_3. *J. Mater. Sci.*, **17** (1982) 2359–66.
2. Sun, W. Y., Yen, T. S. & Tien, T. Y., Subsolidus phase relationships in the system Re–Al–O–N (where Re = rare earth elements). *J. Solid State Chem.*, **95** (1991) 424–9.
3. Sun, W. Y., Huang, Z. K., Tien, T. Y. & Yen, T. S., Phase Relationships in the System Y–Al–O–N. *Mater. Lett.*, **11** (1991) 67–9.
4. Huang Z. K., Tien, T. Y. & Yen, T. S., Subsolidus phase relationships in Si_3N_4–AlN–rare-earth oxide systems. *J. Am. Ceram. Soc.*, **69** (1986) C-241–2.
5. Thompson, D. P., Phase relationships in Y–Si–Al–O–N ceramics. In *Proc. Int. Symp. Tailoring Multiphase and Composite Ceramics*, ed. R. E. Tressler *et al. Mater. Res. Soc. Symp. Proc.* (1986) 93–102.
6. Sun, W. Y., Huang, Z. K. & Chen, J. X., Subsolidus phase relationships in the system Y_2O_3–Al_2O_3:AlN–Si_3N_4. *Trans. Brit. Ceram. Soc.*, **82** (1983) 173–5.
7. Sun, W. Y., Tien, T. Y. & Yen, T. S. (Yan, D. S.), Subsolidus phase relationships in part of the system Si,Al,Y/N,O: the system Si_3N_4–AlN–YN–Al_2O_3–Y_2O_3. *J. Am. Ceram. Soc.* **74** (1991) 2753–8.
8. Mandal, H., Thompson, D. P. & Ekström, T., Heat-treatment of Ln–Si–Al–O–N glasses. In *Proc. 7th Irish Mater. Forum Conf. IMF7*, eds M. Buggy & S. Hampshire. Trans. Tech Publications, Switzerland, 1992, pp. 187–203.
9. Thompson, D. P., New grain-boundary phases for nitrogen ceramics. *Mater. Res. Soc. Symp. Proc.* **287** (1993) 79–92.
10. Cheng, Y.-B. & Thompson, D. P., Aluminium-containing nitrogen melilite phases. *J. Am. Ceram. Soc.*, **77** (1994) 43–8.
11. Wang, P. L., Yu, H. Y., Sun, W. Y., Nygren, M. & Ekstrom, T., Study on the solid solubility of Al in the melilite systems $R_2Si_{3-x}Al_xO_{3+x}N_{4-x}$. *J. Eur. Ceram. Soc.*, **15** (1995), 689–96.
12. Sun, W. Y., Yan, D. S., Gao, L., Mandal, H., Liddell, K. & Thompson, D. P., Subsolidus phase relationships in the systems Ln_2O_3–Si_3N_4–AlN–Al_2O_3(Ln=Nd,Sm). *J. Eur. Ceram. Soc.*, **15** (1995) 349–55.
13. Tu, H. Y., Sun, W. Y., Wang, P. L. & Yan, D. S., Glass forming region in the Sm–Si–Al–O–N system. *J. Mater. Sci. Lett.*, **14** (1995) 1118–22.
14. Sun, W. Y., Wang, P. L. & Yan, D. S., The $\alpha' \rightarrow \beta'$ phase transformation in sialon ceramics by heat treatment. *Mater. Lett.*, **26** (1996) 9–16.